Air-to-Indoor Propagation Measurements with a focus on Low RF-based Navigation

Ignacio Rodriguez*, Melisa López†, Wahyudin P. Syam‡, David Scott‡,
Alejandro Pérez-Conesa‡, Rigas T. Ioannides§
*Department of Electrical Engineering, University of Oviedo, Gijón, Spain, irl@uniovi.es
†Department of Electronic Systems, Aalborg University, Aalborg Øst, Denmark, mll@es.aau.dk
‡GMV NSL, Nottingham, United Kingdom, alejandro.perezconesa@gmvnsl.com
§European Space Agency, ESA-ESTEC, NAV-PFE, Noordwijk, The Netherlands, rigas.ioannidis@esa.int

***Abstract*—Providing global communication, navigation and positioning with outdoor systems might be challenging in indoor and deep indoor situations, due to the limited penetration capabilities of the radio signals into buildings. The use of drones as radio source platforms and low radio frequencies might help alleviate the problem due to improved propagation characteristics in terms of elevation angle and coupling into construction materials. This paper explores air-to-indoor propagation based on an operational proof-of-concept navigation system working at 133, 401.5 and 500 MHz in two different building scenarios. The results demonstrate the favorable radio propagation conditions experienced by the setup, which resulted in viable outdoor transmission of navigation signals into indoor and deep indoor locations.**

***Index Terms*—radio propagation, air-to-indoor propagation, low radio-frequency, drone-based measurements, building penetration loss, navigation.**

I. Introduction

Reliable and accurate communication, positioning and navigation capabilities are an essential demand by first responders in emergency and disaster situations [1]. While current solutions based on global navigation satellite systems (GNSS) allow to provide the desired services in certain situations, global positioning and navigation is still a challenge in indoor, deep indoor scenarios and other challenging scenarios such as street canyons, for example [2]. In this respect, in recent years, a number of technical solutions have been proposed which consider unmanned aerial vehicles (UAV) as system platforms for the support of disaster and emergency communication, due to their versatility, quickness and easiness of deployment [3]. However, such systems typically focus on outdoor-only scenarios, as having a global outdoor and indoor system is still a technical challenge, among other reasons, due to the limited penetration of radio signals into building structures [4]. Furthermore, although there exist extensive literature and models addressing outdoor-to-indoor propagation and building penetration loss (BPL) for terrestrial network systems [5], the availability of literature studies reporting proof-of-concepts or measurements addressing outdoor-to-indoor propagation under the constrains of air-to-ground scenarios with drone-based transmitters remains still quite limited.

In [6], promising results were reported for a radio transmission originated in an UAV and penetrating into a cafeteria and a research building at 4.9 GHz. The authors highlighted that favourable radio conditions have been created by extra reflections due to high elevation angle of the aerial vehicle with respect to the building. The authors in [7] performed a successful outdoor-to-indoor multi-band evaluation at 27 and 38 GHz, emphasizing as well the good propagation conditions from the air. While these studies have focus mainly on the use of typical cellular bands from terrestrial systems such as 4G and 5G, exploiting the capabilities of sub-GHz frequencies might also have a further positive impact on the signal penetration into buildings due to the good propagation properties, as highlighted in [8].

This paper aims at complementing existing literature by reporting the results from an air-to-indoor measurement campaign performed to validate the proof-of-concept of a low radio-frequency (RF) communication and navigation system with extended coverage capabilities [2]. In this case, the focus is put on three low RF frequency bands: 133, 401.5, and 500 MHz, and outdoor-to-indoor measurements were performed in operational system conditions for two types of buildings. While these paper focuses on the radio propagation aspects of the campaign, the navigation signal performance has already been addressed in [9]. The remainder of the paper is structured as follows. Section II describes all aspects related to the measurement campaign including measurement scenarios, setup, test description and data processing. Section III elaborates on the measurement results. Finally, Section IV concludes the paper.

II. Measurement Campaign

A. Measurement Setup

To perform the experimental measurement tests, a low-RF transmitter (TX) - receiver (RX) system was developed. Both the TX and the RX were implemented based on software defined radio (SDR) units. Specifically, the TX was implemented in a portable, battery-powered Ettus USRP E312 [10], and mounted as payload on a DJI Matrice 300 RTK drone [11] as depicted in Fig. 1a. The effective TX antenna height was varying according to the specific flight/hover height of the different tests. The RX was implemented in a powerful Ettus USRP X310 [12] and mounted on a trolley, as shown in

(a) (b)

Fig. 1: Overview of the measurement setup composed of (a) drone-mounted TX, and (b) trolley-mounted RX.

TABLE I: Summary of TX and RX RF configuration

TX	Navigation signal	SS-CDMA + modified GPS L1 C/A [9]
	Signal bandwidth	10 MHz
	TX power	+17 dBm
	TX antenna gain	2.15 dBi
RX	RX antenna gain	2.15 dBi
	RX sensitivity	-110 dBm

Fig. 1b. The RX antenna height was kept constant for all tests at 1.3 m. The antennas used at both TX and RX sides were similar. More specifically, for the tests at 133 MHz were performed with antennas RETEVIS H-777 [13], while the tests at 401.5 and 500 MHz were performed with antennas RETEVIS RT1/3 [14]. Table I summarizes the RX/TX RF configuration utilized throughout the entire measurement campaign.

B. Measurement Scenario

The experimental tests were performed at the Harwell Science and Innovation Campus, United Kingdom. This technological campus area can be classified as sub-urban with a low density of 2-3-storey buildings, single-lane roads, and densely vegetated. In particular, air-to-ground and air-to-indoor measurements were performed at two different building environments: 1) the GMV NSL building, and 2) the Quad One building. An aerial overview of the location of the buildings within the environment together with key measurement reference points are displayed in Fig. 2. The first building, the GMV NSL building, which can be classified as of "traditional" type [5], is a two-floor old building composed of brick and concrete walls of 40 cm thickness. As shown in Fig. 3, the building has multiple windows (24 per floor). Two different types of glass were observed in the windows: 1) BS EN 12150-1 thermally toughened soda lime silicate glass [15], and 2) BS6206 laminated safety glass [16]. The second building, the Quad One, which can be classified as of "thermal-efficient" type [5], is a 3-storey building mainly composed of glass and a steel structure of 36 cm thickness, as shown in Fig. 4. The SGT 1(C)3 EN 14179 glass composing the building façade is a heat soaked thermally toughened soda lime silicate glass [17].

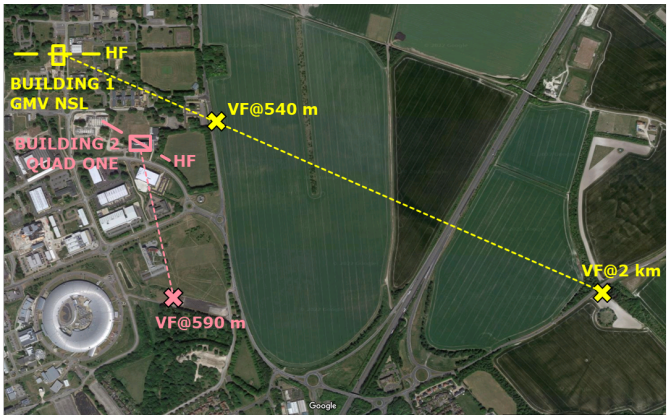

Fig. 2: Overview of the Harwell technological campus, including the two buildings locations at which the experimental tests were conducted, the surroundings, and reference measurement points.

C. Test Description

Two different types of measurement tests were performed:

1) **Horizontal flight (HF) over the target building**: this test was performed in order to analyse the performance of the system under a rapid UAV deployment configuration. An horizontal pass flight over a target building was emulated by hovering the drone equipped with the TX at 13 positions at 40 m height, considering visibility from elevation angles in the range $\alpha = [10°, 170°]$. For the GMV NSL traditional building assessment, outdoor-to-indoor signal propagation was evaluated by locating the RX at 4 different positions: outdoor (90 cm apart from the building façade, next to the main entrance), indoor – ground floor (GF), deep indoor – ground floor, and indoor – first floor, as illustrated in Fig. 3. For the Quad One thermal-efficient building, the RX was located at 2 different positions next to one of the corners of the building: outdoor (90 cm apart from the building façade), and indoor - GF, as described in Fig. 4.

2) **Vertical flight (VF) at long distance from the target building**: this test was done in order to evaluate and validate the operational range of the system by considering multiple TX topologies in terms of different UAV elevations at long distances from the building. In particular drone TX heights of 2.5, 7.5, 20, and 75-110 m were considered at distant locations ranging from 500 m to 2 km from the target buildings where the RX was deployed at. For both buildings, the RX was located at two different positions: outdoor, and indoor - GF, as per Figs. 3 and 4.

All propagation tests were done for the three target low RF carriers frequencies (f): 133, 401.5, and 500 MHz. However, it should be noted that, at the Quad One thermal-efficient building, the measurements were heavily impacted by external interference caused by some RF leakage from the walkie-talkie system used by the Campus employees (operating in the 433 MHz band) and are, thus, not reported in that specific case.

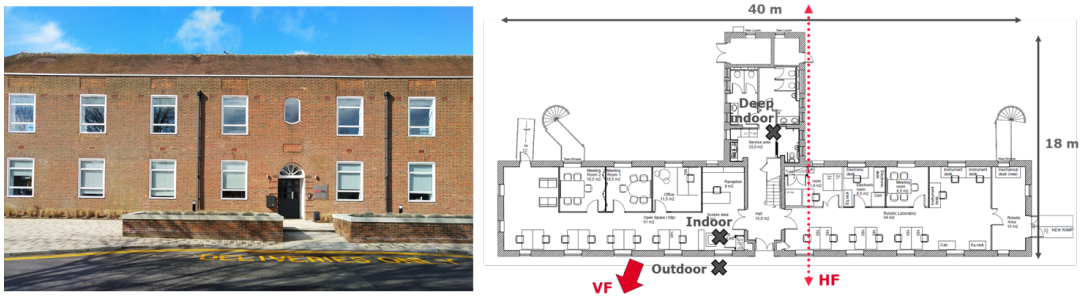

Fig. 3: Overview of the GMV NSL (traditional) building including measurement positions and reference orientations.

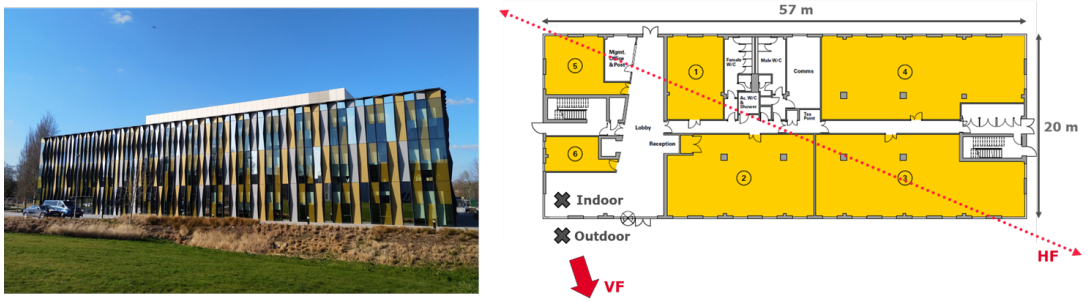

Fig. 4: Overview of the Quad One (thermal-efficient) building including measurement positions and reference orientations.

III. Results and Discussion

First, the measurement results for the HF test at the GMV NSL traditional building are addressed. Fig. 5 presented the received power levels experienced by the RX at the different low RF carrier frequencies at the different outdoor and indoor measurement locations. The observed trends can be explained from the geometry of the TX-RX link at the different elevations. At the outdoor position, TX and RX were in line-of-sight (LOS) in the range 10-60 degrees of elevation, after that, the TX-RX link was shadowed by the building (90 and 120 degrees). There is a small increase in RF power level at 120-130 degrees, probably due to the effective propagation of the signal being through the building instead of above the building. The signal decays afterwards for elevations 140-170 degrees as the TX-RX link distance continues to increase. For the indoor positions, the highest RF levels were observed at the indoor position in the first floor. This was expected as the RX was located nearby the closed window in LOS conditions to the TX for elevations between 10 and 60 degrees. As there was also another window right in the back of the building at this indoor position, the RX RF levels are quite high for the rest of elevations (90-170 degrees) even when the TX was in non-line-of-sight (NLOS). The RF levels are also high for the RX at indoor position in the ground floor up to 160 degrees. This is due to the fact that the RX was deployed in a similar fashion as in the first floor: right behind a window, with LOS conditions in the first part of the HF pass. However, differently from the results at the first floor, at the ground floor, the RF levels decay for elevation angles between 90 and 170 degrees, due to the fact that, despite the layout is similar to the first floor (with a window on the opposite side of the building), the TX-RX link is much more obstructed by the back part of the building itself, resulting in extra shadowing as compared to the first floor, which has much more favourable propagation conditions due to being the highest floor. The RF power levels experienced at the deep indoor position in the ground floor are clearly the lowest when the RX is at elevations between 10 and 60 degrees, flying towards the building. Once the RX reaches close the building (90 degrees elevation) and starts flying away from it (120-170 degrees elevation), the RF levels become comparable to those from the indoor positions. This is due to the low attenuation introduced by the structures of this type of building. The above discussion holds for all the different frequencies. However, the RF signal variability depending on the frequency should be also noted, where the lowest frequency (133 MHz) presented the highest received power values due to the lowest building attenuation. On average, received power levels at 401.5 and 500 MHz were 2 and 6 dB higher than at 133 MHz.

For the Quad One thermal-efficient building, the received power level measurement results for the outdoor and indoor positions are plotted in Fig. 6, for the two successfully-measured carrier frequencies. Differently from the previous case, where the HF was done over a straight line perpendicular to the main façade of the building; in this case, the HF was done over a diagonal straight line over the building. At the outdoor position, TX and RX were in LOS in the range between 10 and 50 degrees of elevation. After that, the TX-RX link was shadowed by the building (from 60 to 120 degrees) becoming almost-line-of-sight (ALOS), partially

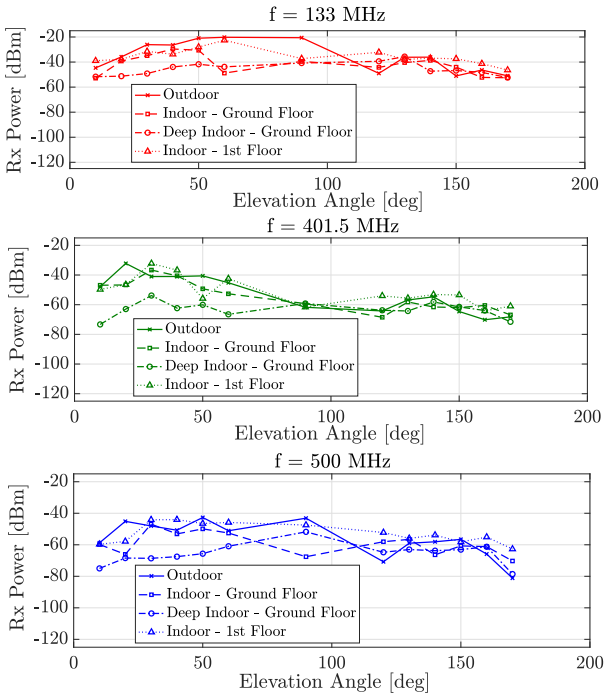

Fig. 5: RX RF power levels measured in the HP test at the traditional building for the different positions at the different frequencies.

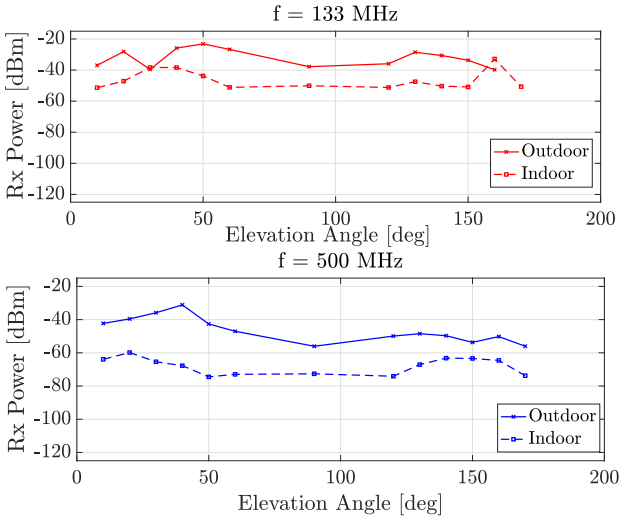

Fig. 6: RX RF power levels measured in the HP test at the thermal-efficient building for the different positions at the different frequencies.

obstructed by some vegetation. In this case, the indoor RF signal levels were consistently much lower than the ones outdoors. This is due to the effect of the thermal-efficient building structure, which introduces higher attenuation than the traditional building structure. On average, received power levels at 500 MHz were 18 dB higher than at 133 MHz.

Finally, the measurement results for the long distance VF test at both buildings are shown in Fig. 7, considering the different building types, carrier frequencies, TX distance to the target building (d_{TX}), and TX heights (h_{TX}). For the two considered distances to the GMV NSL traditional building, the higher the TX was, the better the received RF signal level was. This is due to the geometry of the scenario, as for TX heights of 20 m and higher, the clutter (vegetation and buildings) is avoided, increasing the LOS probability to the considered RX positions. Interestingly, in this traditional building case, when the TX was located at 2 km distance, higher received power levels were observed for the indoor position as compared to the outdoor position at 133 and 401.5 MHz. The difference in power values was 2-4 dB which indicates comparable absolute power contributions to the outdoor and indoor positions probably following different propagation paths (i.e., the signal is coupled into the building to the indoor RX position from a different propagation path than the path serving the outdoor RX position). The long-distance VF test results indicate similar geometry trends as in the traditional building case, with favourable propagation for higher TX heights. This is particularly clear in the 500 MHz case, where due to the high attenuation of the building, no signal was received inside the building, except for the case where the TX was at the highest flight height of 120 m.

The overall variability of received power levels (ΔRF) in the different scenarios is summarized in Table II together with the BPL values estimated from the aerial measurements.

A. Navigation Signal Performance

Although not explicitly addressed in this paper, it is worth mentioning that the same measurements discussed in this study were also used to analyze the performance of the transmitted navigation signal (which was specifically designed for this particular project) in the different described air-to-ground and air-to-indoor propagation situations. Such analysis evaluated the navigation signal transmission success rate for acquisition, tracking and positioning estimation, leading to the overall navigation performance results also summarized in Table II in terms of success rate (NAV-SR). The overall conclusion of the assessment is that the selected signals combined with the choice of low RF carriers and aerial platform demonstrated improved penetration capabilities and abilities to carry navigation information into indoor and deep indoor scenarios. For further reference, a more extensive analysis of the navigation performance assessment is given in [9].

IV. Conclusions

This paper presented an air-to-indoor propagation assessment performed with a transmitter mounted in a drone and receiver deployed at different challenging positions within traditional and thermal-efficient building scenarios. Due to improved propagation conditions low RF carriers were selected for the assessment and evaluation of the system in operational conditions. The observed propagation trends and building penetration loss values, together with the navigation

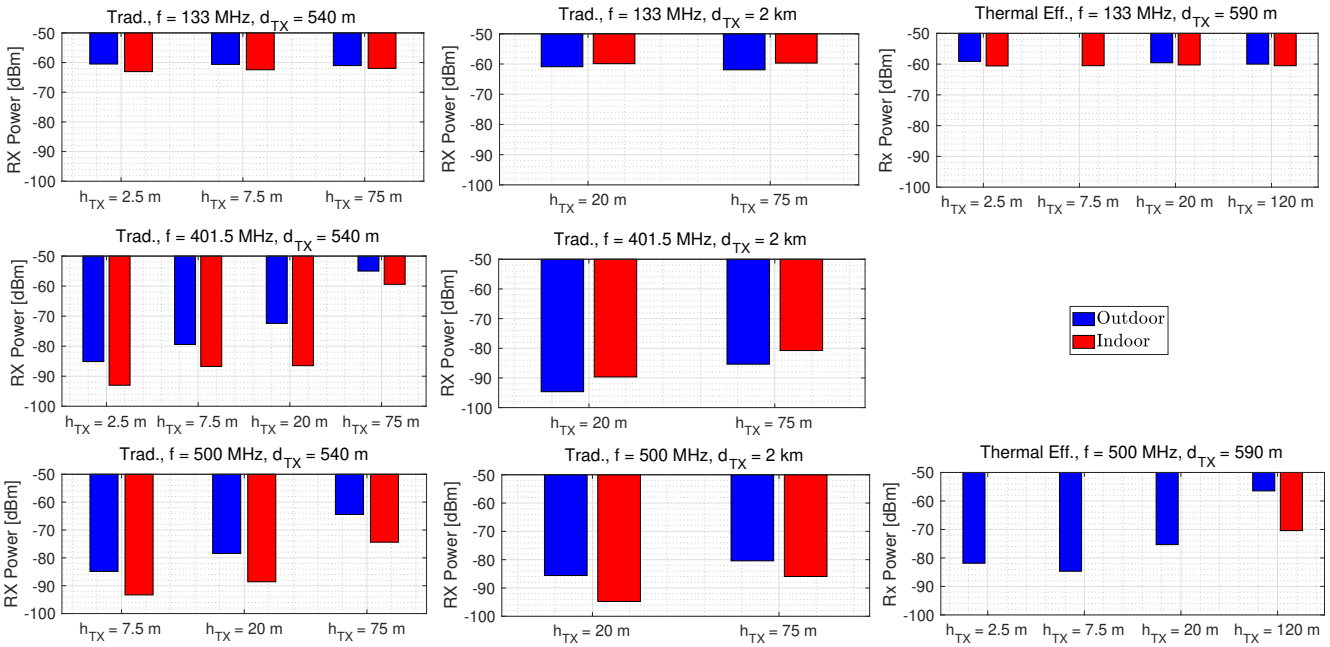

Fig. 7: RX RF power levels measured in the VF test at the traditional and thermal-efficient buildings for the different outdoor and indoor positions at the different frequencies.

signal performance analysis, serve to validate the choice of the drone as an ideal carrier platform and the use of low frequencies (133-500 MHz) for viable navigation system operation, even in certain indoor and deep indoor conditions.

TABLE II: Summary of the overall received power level variability, estimated building penetration loss and navigation signal success rate performance for the different scenarios

	f [MHz]	ΔRF [dBm]	est. BPL [dB]	NAV-SR
traditional	133	-20.2/-61.0	10.4-10.7	83%
	401.5	-32.1/-94.6	10.9-16.0	83%
	500	-42.7/-94.5	8.6-16.9	83%
thermal	133	-23.2/-60.6	15.2-18.1	67%
efficient	500	-31.1/-110	21.0-25.2	54%

ACKNOWLEDGMENT

This work was supported by the European Space Agency NAVISP programme and funded under the activity EL1-018: "Low-RF Fast Deployable Systems for Emergencies in Difficult Environments". Publication work was supported by the Spanish Ministry of Science and Innovation under Ramon y Cajal Fellowship number RYC-2020-030676-I. The authors would like to express their gratitude to David Payne from GMV NSL for his collaboration as drone operator during the experimentation campaign.

REFERENCES

[1] D. G.C., A. Ladas *et al.*, "An overview of post-disaster emergency communication systems in the future networks," *IEEE Wireless Communications*, vol. 26, no. 6, pp. 132–139, 2019.

[2] European Space Agency, "ESA NAVISP EL1-018: Low-RF Fast Deployable Systems for Emergencies in Difficult Environments," Available online: https://navisp.esa.int/project/details/52/show, Accessed on 14 October 2022.

[3] A. Ranjan, B. Panigrahi *et al.*, "A study on pathloss model for uav based urban disaster and emergency communication systems," in *2018 Twenty Fourth National Conference on Communications (NCC)*, 2018, pp. 1–6.

[4] "A survey of radio propagation channel modelling for low altitude flying base stations," *Computer Networks*, vol. 171, p. 107122, 2020.

[5] R. Rudd, J. Medbo *et al.*, "The development of the new itu-r model for building entry loss," in *12th European Conference on Antennas and Propagation (EuCAP 2018)*, 2018, pp. 1–5.

[6] K. Saito, Q. Fan *et al.*, "Outdoor-to-indoor radio propagation loss measurement by using an unmanned aerial vehicle in 4.9 ghz band," in *IEICE Tech. Rep.*, vol. 117, no. 178, 2017, pp. 25–30.

[7] F. Fuschini, M. Barbiroli *et al.*, "Multi-band outdoor-to-indoor propagation measurements using a drone," in *2022 16th European Conference on Antennas and Propagation (EuCAP)*, 2022, pp. 1–4.

[8] A. Boyle and M. E. Tolentino, "Localization within hostile indoor environments for emergency responders," *Sensors*, vol. 22, no. 14, 2022.

[9] A. Perez-Conesa, W. Syam *et al.*, "Low rf-based navigation for emergencies in difficult environments," in *35th International Technical Meeting of the Satellite Division of The Institute of Navigation (ION GNSS+ 2022)*, 2022.

[10] Ettus Research, "USRP E312."

[11] DJI, "DJI Matrice 300 RTK."

[12] Ettus Research, "USRP X310."

[13] RETEVIS, "H-777 dual band 144/430 MHz."

[14] ——, "RT1/3 400-520 MHz."

[15] "BS EN 12150-1:2015+A1:2019 - TC: Glass in building. Thermally toughened soda lime silicate safety glass - Definition and description," British Standards Institution (BSI), Tech. Rep., 2019.

[16] "BS EN 12600:2002: Glass in building. Pendulum test. Impact test method and classification for flat glass," British Standards Institution (BSI), Tech. Rep., 2003.

[17] "BS EN 14179-1:2016 - TC: Glass in building. Heat soaked thermally toughened soda lime silicate safety glass - Definition and description," British Standards Institution (BSI), Tech. Rep., 2016.